

OpFML: Pipeline for ML-based Operational Forecasting

Shahbaz Alvi^{*a}, Giusy Fedele^a, Gabriele Accarino^c, Italo Epicoco^{a,b}, Ilenia Mancò^a, Pasquale Schiano^a

^aCMCC Foundation - Euro-Mediterranean Center on Climate Change, LE, Lecce, Italy

^bDepartment of Innovation Engineering, University of Salento, LE, Lecce, Italy

^cDepartment of Earth and Environmental Engineering, Columbia University, New York, NY, United States of America

Abstract

Machine learning is finding its application in a multitude of areas in science and research, and Climate and Earth Sciences is no exception to this trend. Operational forecasting systems based on data-driven approaches and machine learning methods deploy models for periodic forecasting. Wildfire danger assessment using machine learning has garnered significant interest in the last decade, as conventional methods often overestimate the risk of wildfires. In this work, we present the code **OpFML: Operational Forecasting with Machine Learning**. OpFML is a configurable and adaptable pipeline that can be utilized to serve a machine learning model for periodic forecasting. We further demonstrate the pipeline's capabilities through its application to daily Fire Danger Index forecasting and outline its various features.

Keywords: machine learning, fire danger index, climate scientist, Earth science, ml-based forecasting, wildfires

1. Introduction

Machine learning (ML) methods support research in the field of Climate and Earth Science by leveraging increasingly precise measurements from both in-situ instruments and remote sensing [1, 2]. Among the many areas of application of ML in these fields, it has frequently been used for forecasting the probability of wildfire occurrence in a geographical area. A wildfire is an unplanned, uncontrolled fire that can occur in an area with burnable biomass. The threat of wildfires is expected to increase as climate change creates conditions favorable for wildfire occurrence [3]. In Europe, the weekly cumulative area burned in 2025 due to forest fires is $\approx 189.3\%$ larger than the average from 2006 to 2024 (see the top image of Figure 1). Moreover, the weekly cumulative number of forest fires has increased by $\approx 101\%$ (see the bottom image of Figure 1).

Situational awareness is key to preventing forest fires and, in the event of their occurrence, essential for combating them. The daily Fire Danger Index (FDI) reflects the highest conditional probability of forest fire occurrence within a specific pixel on a given day. By providing insights into how favorable conditions may be for the occurrence of wildfire, the FDI becomes a vital tool for proactive risk assessment.

While a plethora of tools are available to support training, validation, and testing of ML models [5, 6, 7, 8], there is a lack of tools to serve the model for autonomous and periodic forecasting. Such a tool can be useful in several important use cases within the climate community where deploying an ML model at an operational level is desirable. For instance, the potential of ML methods in wildfire management and their comparison with traditional approaches have been studied extensively [9].

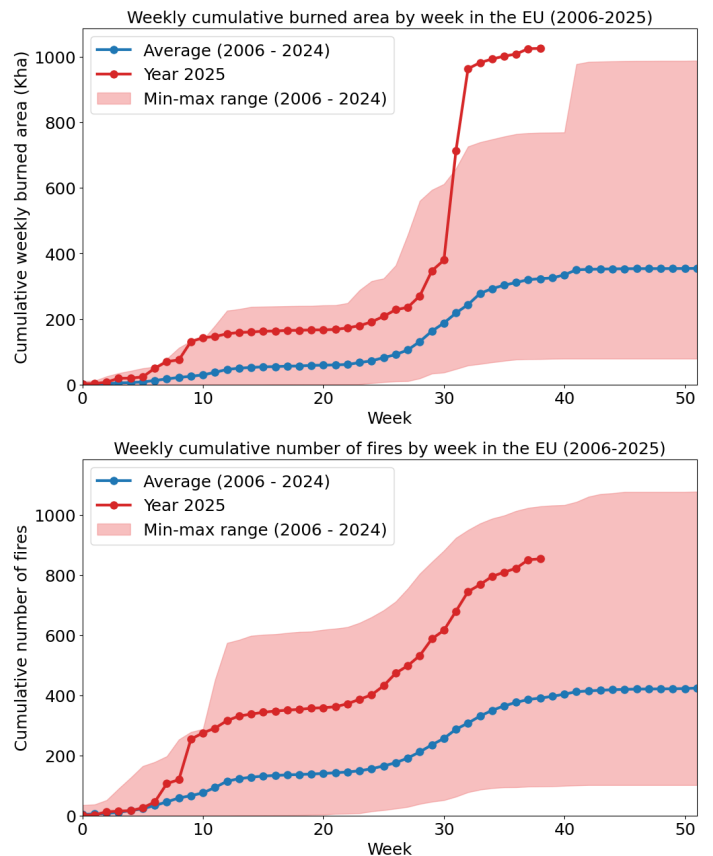


Figure 1: Cumulative burned areas (top) and cumulative number of fires (bottom) in 2025 (until September) compared to the average from 2006 to 2024. Source EFFIS fire alert system [4]

The growing trend of using ML techniques in the assessment of fire danger is motivated by the limited capacity of traditional models to predict wildfire activity and their tendency to overestimate the risk. One of the earliest works using ML methods for predicting forest fire occurrence dates back to the work of [10]. They used an Artificial Neural Network (ANN) trained over the Canadian region to predict fires, taking into account anthropogenic factors such as distance to the nearest roads, towns, and campsites. Soon after, [11] used weather variables as fire predictors for an ANN neural network. A CNN architecture was employed in [12], whereas [13] extended this approach by integrating an LSTM component (ConvLSTM), enabling a more effective representation of time series data. The latter study is particularly relevant, as it applies the same model architecture adopted in the use cases presented in this manuscript.

Considerable efforts have been devoted to demonstrating the potential of machine learning approaches for estimating FDI; however, such applications remain largely at the proof-of-concept stage. A fully operational tool leveraging ML for daily FDI estimation across a geographical region remains underdeveloped. In [14], an operational system was proposed for estimating the fire risk associated with a given day over the geographical region of Galicia in north-west Spain. More recently, [15] explored several aspects of predicting fire activity on a global scale at 1 km resolution. The paper further discusses the performance of the trained model in the context of the European Center for Medium-Range Weather Forecast (ECMWF) data-driven operational fire prediction system.

This work aims to bridge the gap between proof-of-concept application of ML models and practical implementation in operational forecasting systems. We present an operational, adaptable, and flexible pipeline for wildfire forecasting based on data-driven methods. The pipeline's functionality and effectiveness are further demonstrated on a use case Section 3. Demonstrating the tool on test sites highlights its potential for real-world applications. The paper will further demonstrate that the pipeline can be used for use cases other than those presented in this work with minor alterations (see Section 2). The code is freely available through a public GitHub repository¹ [16].

2. Pipeline Layout

2.1. Motivation

The development of the pipeline stemmed from the need to consistently and periodically forecast the daily FDI over a geographic region using an ML model. The pipeline comprises the essential components that ingest and pre-process the latest and updated status from a data store, and execute the integrated ML model to forecast the FDI.

2.2. Structure of the pipeline

2.2.1. Layout

The two main components of the pipeline are the classes `PreProcessing` and `DataStore`. Two TOML (Tom's Obvi-

ous Minimum Language) configuration files are required to execute the pipeline: one for the data store, and the second for each geographic site included in the specific use case. TOML files use a human-readable key–value format in which each section (defined by square brackets) is a dictionary consisting of key–value pairs given under that section; sections can also be nested within other sections. The format supports types like strings, numbers, arrays, and tables. The pipeline layout is summarily depicted in Figure 2.

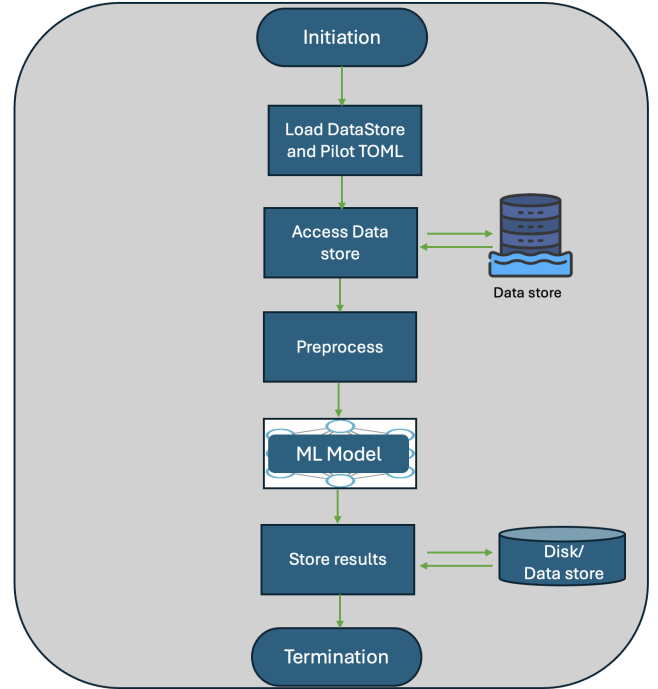


Figure 2: Schematic flow chart of the pipeline.

2.2.2. Data Consumption

The `DataStore` class consumes the data downloaded from the data store. Utilizing ML models to produce periodic forecasts for a target variable requires integrating a data store to consume the latest data. The TOML file serves two purposes: firstly, it stores the parameters for forming the query to access the data from the data store API. It is worthwhile to mention that all variables supported by the pipeline can be configured in the data store TOML file, even if some are not used during the model inference for a target geographical region. Therefore, the data store TOML file serves as a library for all variables that the pipeline can access. Secondly, it also stores the transformations that have to be applied to each variable by the `PreProcessing` class before executing inference (see Section 2.2.3). Although the data store TOML file contains information to retrieve all the variables that can be supported by the pipeline, for a specific geographical region, the pipeline retrieves only the variables that are listed in the TOML file for that geographic region; this file is called the pilot TOML file (see the next section). As an example of how a variable is configured in the data store TOML file, Figure 3 shows the data store TOML entry for consuming the “NDVI” data. The `gathering` subsection for each variable

¹<https://github.com/CMCC-Foundation/opfml>

```
[data.ndvi]
  [data.ndvi.gathering]
    longname="Normalized difference vegetation index"
    source="dds"
    dataset="ndvi-silvanus"
    frequency="puglia"
    variable=["ndvi"]
    format="netcdf"
    var_name=["ndvi"]
    type="dynamic"
    contingency="latest-date"
  [data.ndvi.processing]
    functions=["dataset_resample","fill_time_dimension","interp"]
    kwargs="{'operator':'mean','frequency':'1D','closed':'right','to_lonlat':False}",
    {'dates':dates},
    "None"
```

Figure 3: TOML configuration for the consumption of the NDVI variable. The TOML subsection called “gathering” describes the request to be submitted to the DDS. In the “processing” section, the transformations to be applied to the variable are described together with the input required by each function.

```
[pilot_info]
  datastore="library/datastore.py::DataStore"
  datastore_toml="src/config/data_config.toml"
  preprocessing="library/preprocessing_utils::PreProcessingUtils"
  ndays = 10
  output_dir="pilots/gargano_apulia_it/data/dataset_inference/"
  static_output="pilots/gargano_apulia_it/data/static/"
  xr_grid_file="pilots/gargano_apulia_it/xr_grid.nc"
  pilot_region="gargano"

  [pilot_info.area]
    north = 42.53
    south = 39.44
    east = 19.22
    west = 14.61
```

Figure 4: A section of the pilot TOML file describing the data store class and processing class to be used for the pilot site. Additionally, parameters can also be defined depending on the use case.

includes the parameters required to retrieve the data from the data store. An example of a datastore file is provided in the supplementary material.

The pilot TOML file defines the parameters required for a specific pilot site. Here, the user can describe, among other parameters, the input parameters to initiate the ML model, the DataStore class to be used for this pilot, the geographic boundary box, etc. Most importantly, the variables to be used for inference are listed here they are a subset of the variables in the data store TOML file (more details in Section 2.3). Figure 4 shows a section of the pilot TOML file, while the complete file can be found in the supplementary material.

2.2.3. Data pre-processing

The variables that are consumed from the data store may require further processing before inference. For instance, the ML model adopted for the use case described in this work, the forecast for the daily FDI, does not use the hourly weather forecast, which is consumed from the data store; instead, it requires summary variables derived from the hourly forecast (see D.3). The transformations to be applied to a variable in the data store TOML file are described in the preprocessing section of the variable (see Figure 3). The consumed variables are dynamically transformed, “on the fly”. In the code, the class PreProcessing is responsible for applying the transformations listed in the preprocessing section of each variable. The

```
from xclim.indices import uas_vas_2_sfcwind as sfcwind
import xarray as xr

def compute_wind_speed(self, input: xr.Dataset,
                      var_name_u: str,
                      var_name_v: str):
    output = sfcwind(uas=input[var_name_u],
                      vas=input[var_name_v])
    return output[0].to_dataset()
```

Figure 5: Code snippet of the transformation function in PreProcessingUtils class for computing the wind speed using library xclim, and function uas_vas_2sfcwind. The input xarray Dataset is expected to contain the wind speed components.

class of functions to be used for the preprocessing of the variable is required in the pilot TOML file (see Figure 4). In the code, the class called PreProcessingUtils serves as the library for the transformation functions utilized in the use case demonstrated in this work. An example transformation is illustrated in the code snippet in Figure 5, which calculates the wind speed from the u and v components of the wind speed stored in xarray Dataset. In Appendix A a detailed description is provided that allows users to add new transformations to the PreProcessingUtils class.

2.3. Robustness of the pipeline

The pipeline has been developed keeping flexibility and functionality in mind. Hence, the pipeline can be used for a wide variety of applications other than the one demonstrated in this manuscript. In this section, we describe some of the features that make the pipeline robust and adaptable. Integrating a different ML model is straightforward; one only needs to pass the path of the PyTorch checkpoint file in the pilot TOML file parameters. Different pilot TOML files can accept different ML models. This provides the flexibility to use different ML models in different pilots. Indeed, different ML models could be fine-tuned for optimum performance in that geographical region. The modular structure of the code allows modifications to individual steps of making a forecast with the ML model. As mentioned in Section 2.2.2, the DataStore is configured with the data store used in our use case; however, a different data store can be configured with minimal changes. The required parameters to consume the variables from the data store can be passed through the data store TOML file. In Section 2.2.2, it was highlighted that the datastore class for a given pilot site is defined in the pilot TOML file (see Figure 4). This feature is implemented so that each pilot can use a different data store configured in a separate DataStore class.

A significant bottleneck for the autonomous, periodic inference with ML models is the unavailability of the latest variables in the data store. While for some variables, this poses the risk of critical failure of the pipeline, for other variables, particularly those that vary slowly, the last updated dataset might be sufficient. On the other hand, for cyclic variables, data from the same period in the previous year might suffice. The DataStore class in the code is equipped to handle both these cases, and this option can be enabled for a variable by passing the parameter contingency in the datastore TOML file (see Figure

3). When this parameter is set to `latest-date`, the second-to-lastest available dataset is used in case of failure to retrieve the dataset. If set to `preceding-year` instead, the DataStore class tries to retrieve the data from the previous year. If the `contingency` parameter is not given, no action is taken. In the case of failure to consume data, the pipeline stops with an error.

The specific transformations to be applied to each variable are defined in the preprocessing section of the variable in the datastore TOML file (see Figure 3). The transformation functions are essentially Python functions (see Appendix A) listed in the parameter functions. The parameter `kwargs`, instead, contains the arguments to be passed to each function. The parameters for each transformation are defined in the form of a simple list of strings at the index corresponding to the function functions, making it easy to add new transformations. The entries in `kwargs` follow the standard Python dictionary format for passing parameters to a function. The dictionary is written in string format, making it intuitive to pass the arguments to the function. Moreover, it is also possible to leverage the power of parallel processing within a transformation. The transformations are applied to the data in a cascading sequence, i.e., the first transformation in the list is applied first.

The parser of the input parameters for the transformations (the entries in `kwargs`) has several useful features that are described in detail in the appendix (see Appendix A.1). The transformations used in the use case defined in this work are included in the code; additional transformations can be easily defined by creating a new Python function (see Figure 5 and the appendix for details on how to add new transformations). A distinct "library" of transformation functions can be specified for each pilot in the TOML file, allowing for better management of transformations tailored for each pilot.

As the final word on pipeline robustness, we would like to highlight that although we demonstrate the functionality of the pipeline in a limited scope (see Section 3), the general structure and the adaptable approach of the code make it easy to apply the pipeline to many other use cases in the field of Climate and Earth Science.

3. The daily FDI use case

In this section, we demonstrate the functionality of the pipeline and apply it to the use case of computing the daily FDI. This section outlines information regarding the data used for training, our training methodology, and the ML architecture employed. Moreover, we also present the collection and preprocessing of fire predictors for forecasting the daily FDI for the geographical location in our use case.

3.1. Geographic region

In this section, we describe the geographical regions in which this pipeline will be demonstrated.

3.1.1. Southern Italy

The southern Italian region comprises the provinces of Apulia, Basilicata, the northern parts of Calabria, and the southern part of Campania (shown in Figure 6).



Figure 6: The image shows the south of Italy; namely, the region of Apulia, Basilicata, the southern parts of Calabria, and the northern parts of Campania from the Sentinel-3.

The southern Italian region is recognized as being highly fire-prone. The temperature change throughout the year is gradual and moderate, with July being the warmest month of the year. Like the typical Mediterranean fire season, wildfires are concentrated in the summer months (from June to September). In terms of the total burned area in the year 2024, Apulia accounted for $\approx 10\%$ of Italy's total burned forest area, Calabria standing at 20% contribution [17].

3.1.2. Central Portugal

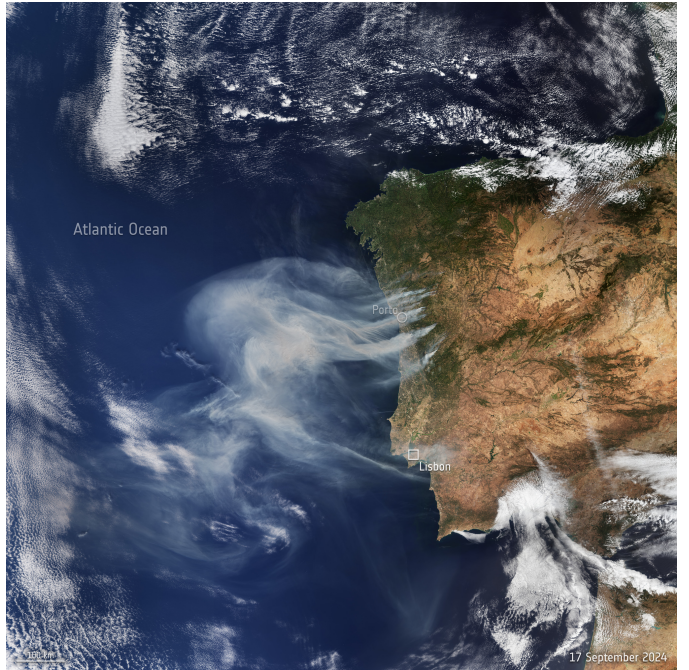


Figure 7: Satellite image over the central Portugal region from the Sentinel-3 showing wildfires in September 2024.

In Portugal, we focus on the central part of Portugal (shown

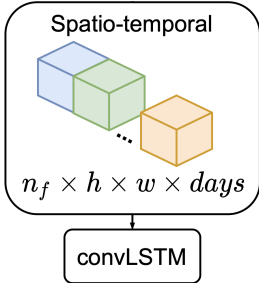


Figure 8: Sample format of a ConvLSTM network. Here, nf is the number of fire predictors, days is the number of days included in the sample, h and w are the size of the area around the fire/no-fire sample. Picture taken from [13].

in Figure 7, where intense and large summer fires have occurred, affecting extensive areas of shrubland and forestland. The terrain topology (with high slopes), the adverse characteristics of the summer weather, and large areas of monoculture forest production regimes, namely Maritime Pine and Eucalyptus, significantly contribute to these intense forest fires. Portugal is generally characterized as having a Mediterranean climate, where the majority of forest fires occur between May and September. Two factors primarily drive forest fires in this region: i) hot and dry summers, and ii) wet and humid falls and winters. These phenomena are further augmented by the vegetation phenology of the region, i.e., growing peak in the Spring, with long hours of sunlight, and the rising temperatures causing accelerated growth of vegetation that is then followed by a dry period in the Summer, thus causing elevated fire hazard.

3.2. ML architecture and training dataset

The ML architecture used to estimate FDI in this work is the Convolutional LSTM (ConvLSTM), following [13]. The model is trained to categorize each pixel on the map as a *fire* or a *no-fire* event and output the respective probabilities, the sum of which is 1. The input format of each sample for the ML model is shown in Figure 8.

We used the dataset prepared and released by the authors of [13] for training our model [18]. The historical fires cover a period of 13 years from 2009 to 2021. The geographic area covered by the dataset includes Greece, parts of Macedonia, Albania, and Turkey.

3.2.1. Fire predictors

The fire predictors used for training and inference are listed in Table 1. These variables were selected based on the analysis presented in [13], which demonstrated their strong correlation with fire occurrence. Except for the Soil Moisture Index (SMI), we have retained all predictors from the analysis of [13]. While the importance of SMI is acknowledged—given its role in indicating vegetation health and fire susceptibility of biomass—it has been excluded due to the lack of continuous data availability, which limits its use in forecasting the daily FDI in our use case.

No.	Variable
1	Normalized difference vegetation index (NDVI)
2	Land surface temperature in daytime
3	Land surface temperature in nighttime
4	Dew point temperature at 2-meter
5	Air temperature at 2-meter
6	Surface pressure
7	Total grid precipitation
8	u&v wind speed components at 10-meters
9	Relative humidity
10	Digital Elevation Model
11	Slope
12	Road distance
13	Waterway distance
14	Population density
15	Corine Land Cover classes

Table 1: Table of fire predictors used to train the daily FDI model. A more detailed table can be found in the appendix.

3.2.2. Data scaling

We standardize the fire predictors on the standard scale for training the model and for inference. The value of a feature F in a pixel is represented in terms of the standard deviation from the mean of the feature in the dataset. Mathematically, for a feature F ,

$$\hat{F} = \frac{F - \langle F \rangle}{\sigma_F} \quad (1)$$

Here, σ_F is the standard deviation of feature values F in the entire dataset, and \hat{F} is the normalized variable.

3.3. Data for daily FDI forecast

Forecasting the daily FDI over a geographic region requires the ingestion of the latest fire predictors. Managing the continuous ingestion and aggregation of fire predictors from different data stores requires a data store. For the use case demonstrated in this work, the DDS (Data Delivery Service) [19] service, developed at the CMCC Foundation (Euro-Mediterranean Center on Climate Change), is configured in the DataStore class. The DDS, deployed and maintained on the CMCC's facilities, automatically synchronizes its index with the parent repositories to ingest the most recent data available (see Table D.3 in the appendix for a full list of fire predictors and their parent repositories). The DDS API is configured in the data store class (see Section 2.2.2) to retrieve the metadata and eventually consume the dataset. In the following subsection, we describe the dataset used for the daily forecast of FDI.

3.3.1. Numerical models for weather forecasting

Short-range high-resolution weather forecasts used for wildfire risk assessment were generated using version 4.2.1 of the Weather Research and Forecasting (WRF) model [20]. More specifically, within this study, we employ a version of the WRF model configured at ≈ 2 km horizontal resolution ([21], hence referred to as WRF_2km@CMCC) to generate the weather

forecasts used in the pipeline demonstration. Configuration details and the sensitivity analysis that guided parameter choices are reported in WRF_2km@CMCC (also summarized in Table C.2). The forecasting system is configured to produce daily operational 72-hour forecasts at hourly resolution, providing the set of variables required for fire-danger computations (see Appendix, Table D.3) over the regions of interest (Figure 9). Two global forcings were tested for the limited-area WRF setup: NCEP’s Global Forecast System (GFS) and ECMWF’s Integrated Forecasting System (IFS). An in-depth evaluation was first performed with IFS-forced runs over the Apulia region (April–October, 2019–2020), followed by a comparative assessment of GFS- and IFS-forced outputs. Key diagnostics, hourly 2-m temperatures (max/mean/min), 10-m wind speed, and total daily precipitation, were compared against available reference data depending on the study area. A preliminary comparison showed broadly comparable performance between the two forcings; because IFS boundary data are routinely available with an approximate three-day delay, GFS was selected for operational implementation. Following the selection of GFS forcing, WRF_2km@CMCC GFS-driven runs were validated over the pilot sites using both gridded and in-situ observational sources on a case-by-case basis. Validation combined standard statistical diagnostics (e.g., mean bias, rmse; here not shown) with targeted temporal and spatial comparisons to capture both variability and patterns’ distribution. Across the test sites, the GFS-driven simulations demonstrated good performance compared to observational data and adequate performance for fire-weather and fire-risk applications, supporting their use in the operational workflow. Over Italy, the following datasets have been used: (i) the E-OBS [22] gridded observational dataset providing daily atmospheric variables at ≈ 11 km resolution, based on in situ measurements; (ii) in situ weather stations provided by institutions (Agenzia Regionale Attività Irrigue e Forestali - ARIF); (iii) the dataset VHR-REA_IT, a high-resolution dataset derived from dynamically downscaling ERA5 with the COSMO-CLM model, offering hourly data at 2.2 km resolution over the Italian Peninsula [23, 24]. For Portugal, E-OBS gridded data were used once again to evaluate model performance. The gridded reference datasets were selected based on the following criteria: (i) their availability as open-access data; (ii) their widespread use within the scientific community; (iii) their horizontal resolution; and (iv) coverage of the entire areas of interest over the investigated period. Additionally, the network of weather stations provides essential local information, serving as a primary reference for various applications. Model performance was statistically evaluated, demonstrating comparable performance between GFS- and IFS-driven simulations, and strong agreement between WRF_2km@CMCC and the reference datasets (not shown here), supporting its use in fire danger and fire weather risk assessments. The results related to the model skills for both configurations (IFS- and GFS-driven) over the past period demonstrated that both configurations may be used for operational purposes. Nevertheless, among them, only GFS serves as a continuously available operational data source that provides, in near real time, the forcing fields required for dynam-

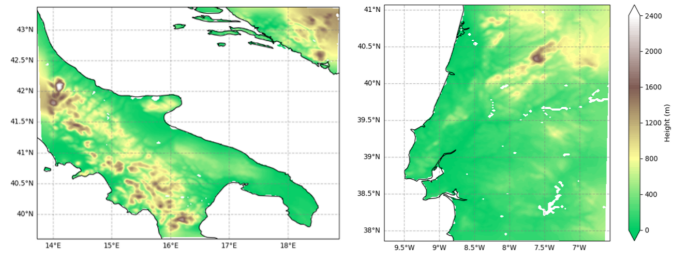


Figure 9: Simulated domains for the three pilot areas: (left) Southern Italy, and (right) Central Portugal.

ical downscaling with WRF_2km@CMCC, whereas IFS forcing has a 3-day delay (Figure C.16 in the appendix shows a simplified overview of the operational WRF_2km@CMCC)

3.3.2. EO Observables

Normalized Difference Vegetation Index: The Normalized Difference Vegetation Index (NDVI) is a widely used index for assessing vegetation condition, vigor, and dynamics. For daily FDI, NDVI is important as it identifies the availability of biomass in different regions. In this work, NDVI from MOD13A2 V6.1 [25], natively on a 16-day temporal resolution at 1 km spatial resolution.

Land surface temperature for night and day: Land Surface Temperature (LST) accounts for the skin temperature as measured by the satellite. The temperature measured during the day (night) corresponds to the daytime (nighttime) LST. We ingest the LST data from the NASA MODIS satellite product, which directly provides the day and night measurements of LST [26] at 1 km daily resolution.

Digital Elevation model and Slope: The Copernicus DEM represents the elevation of the surface of Earth [27]. The slope is derived from the DEM dataset using GDAL library [28].

Corine Land Cover: CORINE Land Cover (CLC) is a consistent, high-resolution land cover and usage information that is managed under the Copernicus Land Monitoring Service. CLC is widely used for environmental monitoring, planning, and modeling applications [29].

3.3.3. Non-EO Observables

Population density, distance to roads and waterways: The model uses population density, distance to the nearest road, and waterways as fire predictors. These datasets are obtained from WorldPop.org and are used without further processing (see [30, 31] for more details on how these datasets are derived).

3.4. Running the pipeline for daily FDI

In this section, we demonstrate how a user can run the pipeline for the use case presented in this work. The input data to make the forecast, presented in Section 5, is provided in the repository. The user can directly execute inference with the provided model with the following command in the terminal executed from the repository’s home directory.

```
python src/inference.py
--conf=pilots/gargano_apulia_it/setup.toml
--date 2024-07-09 --geojson --netcdf
```

With the above command, the daily FDI data will be stored in GeoJSON and `xarray` netCDF format. If data consumption and preprocessing are required, the relevant arguments should be passed in the command line.

```
python src/inference.py
--conf=pilots/gargano_apulia_it/setup.toml
--date 2024-07-09 --collect_data
--prepare_static --save_input
--geojson --netcdf
```

The option `--save_input` stores the data as netCDF file before doing the inference for analysis. `--prepare_static` variables, which are labeled as `static` in the datastore TOML file (see Figure 3), are consumed, processed, and stored to avoid downloading static variables every time a daily forecast is made. More detailed information about setting up the environment and running the pipeline is provided in the git repository [16].

4. Deployment of the pipeline

The pipeline can be containerized using Docker and deployed on a cluster orchestration platform such as Kubernetes, enabling autonomous execution for periodic FDI forecasting. The Docker file provided in the GitHub repository is ready for use and includes all the necessary dependencies required to run the pipeline.

5. Results and Validation

In this section, we present the forecast of the daily FDI produced by the pipeline presented in this paper. The pipeline had been used on two different pilot sites: Southern Italy and central Portugal (see Section 3.1.2 and 3.1.1). In Figure 10, we show the fire danger class for southern Italy, along with the location of confirmed fires marked in the image. In the figure below, the lowest fire danger category, corresponding to category 1, is suppressed for better visualization of the map. A similar plot for the fires in the central Portugal region is shown in Figure 11 for some days in September 2024. We selected some days from the 2024 Mediterranean wildfires when fires were detected in the region of interest. Fire events in this period were selected from the NASA Visible Infrared Imaging Radiometer Suite (VIIRS) dataset at 1 km resolution [32]. The fire anomaly detection is reported in three confidence categories, denoted by integer values 7 (lowest: mostly solar glare), 8, and 9 (highest: pixel saturation). We select events only in the categories of 8 and 9. It is crucial to highlight that not every event in categories 8 and 9 in the VIIRS data might be an actual forest fire. This is because anomalies in VIIRS are recorded if the temperature fluctuation on a pixel is considerably higher than that of the surrounding pixels, without specific attention to the source (such as forest

fires). Therefore, the temperature anomalies identified in the VIIRS dataset are further cross-validated against the MODIS Burned Area Product [33] and only cross-validation events are shown.

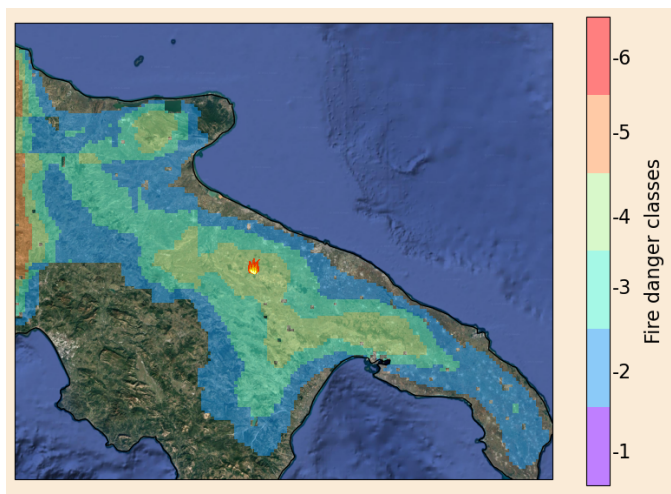
Given the inherent stochastic nature of forest fires, primarily due to human activity, directly comparing the FDI with the occurrence of fire events at a specific location and day is not straightforward. Furthermore, the burned area date in the MODIS burned area data carries an uncertainty of a few days. The comparison adopted in this work takes the maximum of the FDI in each pixel within the days equal to the maximum uncertainty in the MODIS burned area data for that day.

The generalization of ML models beyond the geographic region on which they have been trained remains an open research question. Indeed, the ML models are generally used in fairly controlled conditions when performing inference. Moreover, validating the FDI forecast of an ML model remains a complex task due to the random nature of forest fires and the uncertainty of forest fire detection with remote sensing methods. Therefore, validating “how well the daily FDI correlates with actual fire events” remains a complex question. The authors aim to explore this question regarding the validation of the daily FDI model generalization and validation in future work. Instead, this manuscript primarily focuses on presenting the idea behind the framework and disseminating the code, which could be useful for an automated data-driven forecasting system, in particular, but not limited to, the daily FDI over a geographic region with a model trained in Pytorch Lightning. A detailed validation and performance assessment of the model is out of the scope of this paper.

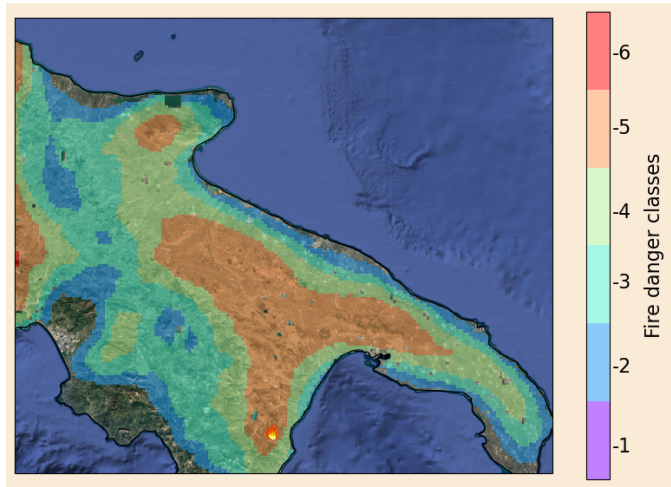
6. Discussion

Much work has been done in the last decade on exploring ML methods in the field of Climate and Earth Sciences. Several studies have shown the utility of using ML methods compared to traditional methods. Utilizing ML models to produce a periodic forecast for a target variable requires integrating a data store to consume the latest predictors for the use case, harmonizing the variables to a standard benchmark, preprocessing the variables, consolidating them into a data structure, and ultimately performing inference for the forecast. Writing such a pipeline from scratch is a daunting task, and there are only a few standard solutions for it. In this manuscript, we present a flexible and adaptive pipeline that can be easily deployed across a variety of use cases in the field of Climate and Earth Sciences. The pipeline is implemented entirely in Python, which is currently the most widely used programming language for ML applications, based on an ML model trained using the Pytorch Lightning tool.

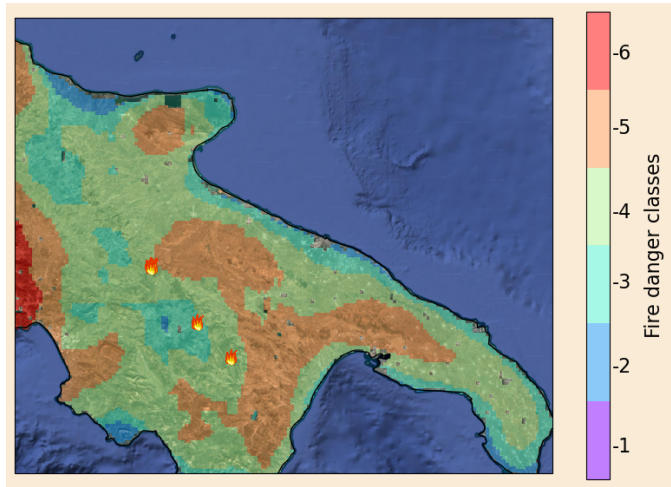
We have further demonstrated the functionality of the pipeline by forecasting the daily FDI over two different geographical regions: Southern Italy and central Portugal, after briefly outlining our training and data preparation methods. At the end, the forecasts of daily FDI produced by the pipeline for the two geographic regions considered are shown and compared with confirmed fire events.



(a) 9th of July 2024.

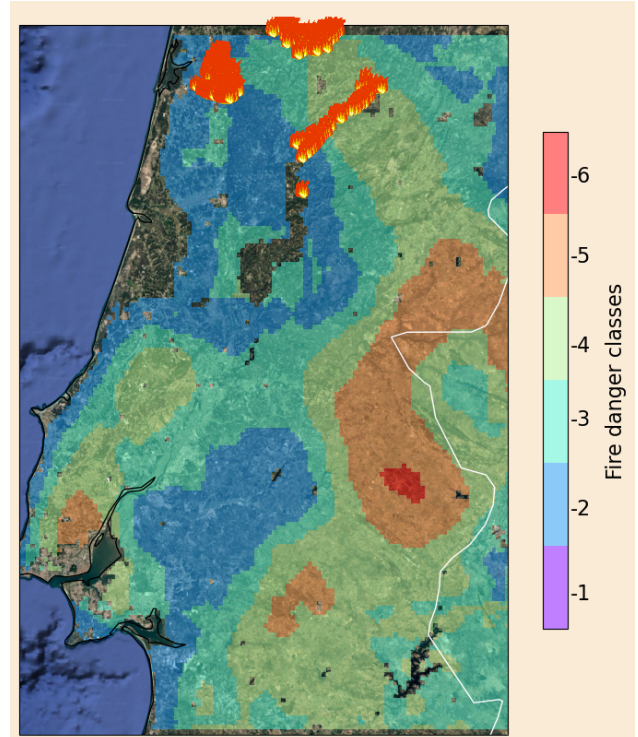


(b) 17th of July 2024.

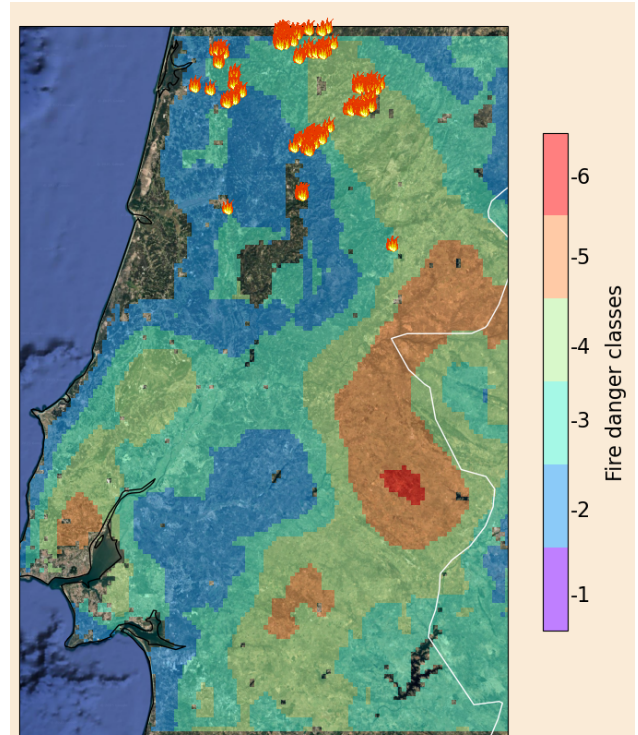


(c) 1st of August 2024.

Figure 10: Daily FDI over southern Italy for some days in July and August of 2024. A fire icon marks the confirmed fire events on that day.



(a) 17th of September 2024.



(b) 20th of September 2024.

Figure 11: Daily FDI over central Portugal for some days in September of 2024. A fire icon marks the confirmed fire events on that day.

The pipeline was developed for the SILVANUS project [34] to produce the daily FDI forecast for various pilot sites. SILVANUS is a Horizon 2020 Green Deal Project, whose main objective was to create a climate-resilient forest management platform to prevent and combat forest.

For the automated computation of the daily FDI for each pilot site, the code was dockerized and deployed on a Kubernetes cluster, demonstrating that it can be deployed for autonomous operation in an orchestration environment.

The challenging task of validating an ML model for forecasting daily FDI is an open area of research. In this manuscript, the authors aim to demonstrate the functionality of the pipeline and disseminate the pipeline code, which can be beneficial for the ML community in the field of Climate and Earth Science. Detailed validation of the model used in this work is out of the scope, and it will be explored in a future paper.

7. Conclusion

The pipeline presented in this work aims to facilitate researchers and developers in the ML community, especially those in the field of Climate and Earth Science. The pipeline aims to bridge the gap between the development of ML models for climate fields and their deployment on the operational level to enable periodic forecasting. Although this work demonstrates the pipeline for the use case of daily FDI, the general structure of the pipeline can serve a variety of use cases in the field of Climate, Earth Sciences, and beyond.

8. Acknowledgments

The authors acknowledge, with gratitude, the constant support of the development team of the CMCC DDS service (Gabriele Tramonte and Valentina Scardigno) throughout the development of this work. This project is partially funded by the European Union’s Horizon 2020 research and innovation program under grant agreement No 101037247.

References

- [1] C. O. de Burgh-Day, T. Leeuwenburg, Machine learning for numerical weather and climate modelling: a review, *Geoscientific Model Development* 16 (22) (2023) 6433–6477. [doi:10.5194/gmd-16-6433-2023](https://doi.org/10.5194/gmd-16-6433-2023).
- [2] A. Bracco, J. Brajard, H. A. Dijkstra, P. Hassanzadeh, C. Lessig, C. Monteleoni, Machine learning for the physics of climate, *Nature Reviews Physics* 7 (1) (2025) 6–20.
- [3] S. C. Coogan, F.-N. Robinne, P. Jain, M. D. Flannigan, Scientists’ warning on wildfire — a canadian perspective, *Canadian Journal of Forest Research* 49 (9) (2019) 1015–1023. [doi:10.1139/cjfr-2019-0094](https://doi.org/10.1139/cjfr-2019-0094).
- [4] C. E. M. S. EFFIS, *Effis statistics portal*, accessed: 2025-10-07 (2025).
URL <https://forest-fire.emergency.copernicus.eu/apps/effis.statistics>
- [5] A. Paszke, S. Gross, F. Massa, A. Lerer, J. T. Bradbury, G. Chanan, T. Killeen, Z. Lin, N. Gimelshein, L. Antiga, A. Desmaison, A. Köpf, E. Yang, Z. DeVito, M. Raison, A. Tejani, S. Chilamkurthy, B. Steiner, L. Fang, J. Bai, S. Chintala, Pytorch: An imperative style, high-performance deep learning library, *neurIPS 2019* (2019).
- [6] M. Abadi, A. Agarwal, P. Barham, E. Brevdo, Z. Chen, C. Citro, G. S. Corrado, A. Davis, J. Dean, M. Devin, S. Ghemawat, I. Goodfellow, A. Harp, G. Irving, M. Isard, Y. Jia, R. Jozefowicz, L. Kaiser, M. Kudlur, J. Levenberg, D. Mane, R. Monga, S. Moore, D. Murray, C. Olah, M. Schuster, J. Shlens, B. Steiner, I. Sutskever, K. Talwar, P. Tucker, V. Vanhoucke, V. Vasudevan, F. Viagas, O. Vinyals, P. Warden, M. Wattenberg, M. Wicke, Y. Yu, X. Zheng, *Tensorflow: Large-scale machine learning on heterogeneous distributed systems*, arXiv preprint arXiv:1603.04467, software available from tensorflow.org (2016).
URL <https://arxiv.org/abs/1603.04467>
- [7] F. Chollet, et al., Keras: The python deep learning library, *Astrophysics Source Code Library* ascl:1806.022, software available from keras.io (2018).
- [8] J. Walczak, M. Mancini, S. Alvi, *Kit4dl: Towards fast prototyping and experimentation in machine learning and deep learning*, *SoftwareX* 26 (2024) 101707. [doi:https://doi.org/10.1016/j.softx.2024.101707](https://doi.org/10.1016/j.softx.2024.101707).
URL <https://www.sciencedirect.com/science/article/pii/S2352711024000785>
- [9] P. Jain, S. C. Coogan, S. G. Subramanian, M. Crowley, S. Taylor, M. D. Flannigan, *A review of machine learning applications in wildfire science and management*, *Environmental Reviews* 28 (4) (2020) 478–505. [arXiv:https://doi.org/10.1139/er-2020-0019](https://doi.org/10.1139/er-2020-0019), [doi:10.1139/er-2020-0019](https://doi.org/10.1139/er-2020-0019).
URL <https://doi.org/10.1139/er-2020-0019>
- [10] C. Vega-Garcia, Applying neural network technology to human-caused wildfire occurrence prediction, *AI Applications* 10 (1996) 9–18.
- [11] A. Alonso-Betanzos, O. Fontenla-Romero, B. Guijarro-Berdiñas, E. Hernández-Pereira, J. Canda, E. Jiménez, J. L. Legido Soto, S. Muñiz, C. Paz-Andrade, M. Paz-Andrade, A neural network approach for forestal fire risk estimation., in: *Proceedings of ECIA*, 2002, pp. 643–647.
- [12] G. Zhang, M. Wang, K. Liu, Deep neural networks for global wildfire susceptibility modelling, *Ecological Indicators* 127 (2021) 107735. [doi:https://doi.org/10.1016/j.ecolind.2021.107735](https://doi.org/10.1016/j.ecolind.2021.107735).

[13] S. Kondylatos, I. Prapas, M. Ronco, I. Papoutsis, G. Camps-Valls, M. Piles, M.-A. Fernandez-Torres, N. Carvalhais, Wildfire danger prediction and understanding with deep learning, *Geophysical Research Letters* 49 (17) (2022). [doi:
https://doi.org/10.1029/2022GL099368](https://doi.org/10.1029/2022GL099368).

[14] A. Alonso-Betanzos, O. Fontenla-Romero, B. Guijarro-Berdiñas, E. Hernández-Pereira, M. Inmaculada Paz Andrade, E. Jiménez, J. Luis Legido Soto, T. Carballas, An intelligent system for forest fire risk prediction and fire fighting management in galicia, *Expert Systems with Applications* 25 (4) (2003) 545–554.

[15] F. Di Giuseppe, J. McNorton, A. Lombardi, et al., Global data-driven prediction of fire activity, *Nature Communications* 16 (2025) 2918. [doi:
10.1038/s41467-025-58097-7](https://doi.org/10.1038/s41467-025-58097-7).

[16] C. Foundation, **Opfml: Operational forecasting with machine learning**, GitHub repository, accessed: 2025-10-08 (2025).
URL <https://github.com/CMCC-Foundation/opfml>

[17] R. P. U. Statistico, **Ispra - incendi forestali: gennaio-luglio 2024**, Online, accessed: 2025-10-07 (2024).
URL <https://protezionecivile.regione.puglia.it/web/ufficio-statistico/-/ispra-incendi-forestali.-gennaio-luglio-2024>

[18] I. Prapas, S. Kondylatos, I. Papoutsis, **Firecube: A daily datacube for the modeling and analysis of wildfires in greece** (2022). [doi:
10.5281/zenodo.6475592](https://doi.org/10.5281/zenodo.6475592)

[19] ADIC-CMCC, **Data delivery system**, accessed: 2025-10-06 (2025).
URL <https://dds.cmcc.it/>

[20] W. C. Skamarock, J. B. Klemp, J. Dudhia, D. O. Gill, Z. Liu, A description of the advanced research wrf model version 4.3, Tech. rep., Open Sky Repository (2021).

[21] I. Manco, C. De Lucia, F. Repola, G. Fedele, P. Mercogliano, A comparative performance study of wrf, cosmo and icon atmospheric models for the italian peninsula at very high resolution, *Tethys: Revista de Meteorología y Climatología Mediterránea* 20 (20) (2023) 1–20.

[22] R. Cornes, G. van der Schrier, E. J. M. van den Bessehaar, P. Jones, An ensemble version of the e-obs temperature and precipitation data sets, *Journal of Geophysical Research: Atmospheres* 123 (2018) 9391–9409. [doi:
10.1029/2017JD028200](https://doi.org/10.1029/2017JD028200).

[23] M. Raffa, A. Reder, G. F. Marras, M. Mancini, G. Scipione, M. Santini, P. Mercogliano, Vhr-re_a_it dataset: Very high resolution dynamical downscaling of era5 reanalysis over italy by cosmo-clm, *Data* 6 (2021) 8. [doi:
10.3390/data6020008](https://doi.org/10.3390/data6020008).

[24] M. Raffa, M. Adinolfi, A. Reder, G. F. Marras, M. Mancini, G. Scipione, M. Santini, P. Mercogliano, Very high resolution projections over italy under different cmip5 ipcc scenarios, *Scientific Data* 10 (2023) 238. [doi:
10.1038/s41597-023-02151-1](https://doi.org/10.1038/s41597-023-02151-1).

[25] K. Didan, **MODIS/Terra Vegetation Indices 16-Day L3 Global 1km SIN Grid V061**, accessed: 2025-10-06 (2021). [doi:
10.5067/MODIS/MOD13A2.061](https://doi.org/10.5067/MODIS/MOD13A2.061).
URL <https://doi.org/10.5067/MODIS/MOD13A2.061>

[26] Z. Wan, S. Hook, G. Hulley, **MODIS Land Surface Temperature Products: MOD11A1/MYD11A1, 1 km, Daily, Daytime and Nighttime**, NASA LP DAAC, USGS/Earth Resources Observation and Science (EROS) Center, accessed: 2025-10-07 (2015). [doi:
10.5067/MODIS/MOD11A1.006](https://doi.org/10.5067/MODIS/MOD11A1.006).
URL <https://doi.org/10.5067/MODIS/MOD11A1.006>

[27] ESA, Copernicus digital elevation model (glo-30 and glo-90), global 30 m & 90 m resolution, Copernicus DEM Release 2023_1, accessed: 2025-10-07 (2023). [doi:
10.5270/ESA-c5d3d65](https://doi.org/10.5270/ESA-c5d3d65).

[28] GDAL/OGR contributors, **GDAL/OGR Geospatial Data Abstraction software Library**, Open Source Geospatial Foundation (2025). [doi:
10.5281/zenodo.5884351](https://doi.org/10.5281/zenodo.5884351).
URL <https://gdal.org>

[29] EEA, Corine land cover (clc) 2018, version 2020_20u1, Copernicus Land Monitoring Service (CLMS) (2020). [doi:
10.2909/CLMS-CLC2018](https://doi.org/10.2909/CLMS-CLC2018).

[30] D. Woods, T. McKeen, A. Cunningham, R. Priyatikanto, A. Sorichetta, A. J. Tatem, M. Bondarenko, Worldpop high resolution, harmonised annual global geospatial covariates. version 1.0, University of Southampton, Southampton, UK, accessed: 2025-10-07 (2024). [doi:
10.5258/SOTON/WP00772](https://doi.org/10.5258/SOTON/WP00772).

[31] C. T. Lloyd, H. Chamberlain, D. Kerr, G. Yetman, L. Pistolesi, F. R. Stevens, A. E. Gaughan, J. J. Nieves, G. M. Hornby, K. MacManus, P. Sinha, M. Bondarenko, A. Sorichetta, A. J. Tatem, Global spatio-temporally harmonised datasets for producing high-resolution gridded population distribution datasets, *Big Earth Data* 3 (2) (2019) 108–139. [doi:
10.1080/20964471.2019.1625151](https://doi.org/10.1080/20964471.2019.1625151).

[32] W. Schroeder, P. Oliva, L. Giglio, I. A. Csiszar, The new viirs 375 m active fire detection data product: Algorithm description and initial assessment, *Remote Sensing of Environment* 143 (2014) 85–96. [doi:
10.1016/j.rse.2013.12.008](https://doi.org/10.1016/j.rse.2013.12.008).

[33] L. Giglio, L. Boschetti, D. P. Roy, M. L. Humber, C. O. Justice, The collection 6 modis burned area mapping algorithm and product, *Remote Sensing of Environment* 217 (2018) 72–85.

- [34] SILVANUS, *Silvanus – integrated technological and information platform for wildfire management*, <https://silvanus-project.eu/>, accessed: 2025-10-08 (2024). URL <https://silvanus-project.eu/>
- [35] S. Baek, *A revised radiation package of g packed mcica and two-stream approximation: Performance evaluation in a global weather forecasting model*, Journal of Advances in Modeling Earth Systems 9 (2017). doi:10.1002/2017MS000994. URL <https://doi.org/10.1002/2017MS000994>
- [36] F. Lott, M. J. Miller, *A new subgrid-scale orographic drag parameterization: Its formulation and testing*, Quarterly Journal of the Royal Meteorological Society 123 (537) (1997) 101–127. doi:10.1002/qj.49712353704.
- [37] T. Yamada, S. Joshi, *A second-order closure model for the prediction of the atmospheric boundary layer*, Journal of the Meteorological Society of Japan 67 (2) (1989) 391–400. doi:10.2151/jmsj1965.67.2_391.
- [38] Y. Xue, J. Shukla, S.-K. Min, *The simplified simple biosphere model (ssib) for land surface process modeling*, Geophysical Research Letters 18 (5) (1991) 899–902. doi:10.1029/91GL00468.
- [39] O. Arino, P. Ramos, J. Jose, V. Kalogirou, S. Bontemps, P. Defourny, E. Van Bogaert, *Global land cover map for 2009 (globcover 2009)*, PANGAEA (2012). doi:10.1594/PANGAEA.787668. URL <https://doi.org/10.1594/PANGAEA.787668>

Appendix A. Transformations of consumed variables

Appendix A.1. How to add new transformations in PreProcessingUtils

Transformations are essentially Python functions that take as input the `xarray` dataset and perform some transformations to the dataset. In Figure 5, we have shown an example of a transformation that takes as an input a `xarray` dataset that contains the `u` and `v` components of the wind velocity and computes the wind speed. The first argument of any transformation function should be `self`, and the second must be `input`. Afterward, any number of arguments can be defined in the transformation like a standard Python function. The names of the arguments in the function must be the same as those passed in the datastores TOML files for the variable, as shown in Figure 3. As in a standard Python function, the order of the arguments is not important. In the following subsection, we explain some useful features of the transformations in the `PreProcessing` class.

Appendix A.2. Using other variables as input for transformation

We will show how a consumed variable can be used to compute other variables. In Figure A.13, we show how the Digital Elevation Model (DEM) is used to compute the variable slope. The input for function `compute_slope` is the DEM variable

already retrieved from the DDS and stored in a local variable (see Figure A.12). The function `compute_slope` is defined with the same format described in the previous section (shown in Figure A.13 for reference). When passing the arguments to the function `compute_slope`, the input parameter is named as `variable`, which signals the `PreProcessing` class that the input to this function is the variable named `dem`, which has already been consumed and stored locally (see Figure A.12).

```
[data.dem]
  [data.dem.gathering]
    longname="Digital Elevation Model"
    source="dds"
    dataset="era5-downscaled-over-italy"
    frequency="portugal"
    variable=["HGT"]
    format="netcdf"
    var_name=["DEM"]
    type="static"
  [data.dem.processing]
    functions=["cdo_remap","interp"]
    kwargs=["None","{'rename':{'HSURF':'DEM'}}"]

[data.slope]
  [data.slope.gathering]
    source="derived:dem"
    type="static"
    var_name=["SLOPE"]
  [data.slope.processing]
    functions=["compute_slope","interp"]
    kwargs=["{'variable':'dem'}","{'rename':{'Band1':'SLOPE'}}"]
```

Figure A.12: Computing slope from the DEM variable that is already ingested from DDS. The picture also shows the entry for consuming the DEM variable from the DDS.

```
def compute_slope(self, input: xr.Dataset):
    input.to_netcdf("./tmp/slope_input.nc")
    gdal.DEMProcsnsing(
        destName="./tmp/slope_output.nc",
        srcDS="./tmp/slope_input.nc",
        processing="slope",
        scale=111120,
        trigonometric=True,
        zeroForFlat=True,
    )
    os.remove("tmp/slope_input.nc")
    return xr.open_dataset("tmp/slope_output.nc")
```

Figure A.13: Function to compute slope from the consumed variable. The input parameter is configured automatically by the pipeline.

Appendix A.3. Passing datastore local variables to the transformation function

An instance of the `datastore` class is passed to the `PreProcessing` class upon initiation. This can be exploited to use the local variables of the `datastore` class in the transformation functions. When passing parameters to a transformation function, the parser of the `kwargs` (see, for example, Figure A.12 and 3) checks if the input parameter is a local variable in

```
[data.ndvi]
[data.ndvi.gathering]
  longname="Normalized difference vegetation index"
  source="dds"
  dataset="ndvi-silvanus"
  frequency="uglia"
  variable=["ndvi"]
  format="netcdf"
  var_name="ndvi"
  type="dynamic"
  contingency="latest-date"
[data.ndvi.processing]
  functions=["dataset_resample","fill_time_dimension","interp"]
  kwargs=[{"operator":'mean','frequency':1D,'closed':right,'to_lonlat':False},
  {"dates":dates},
  "None"]
```

Figure A.14: Entry in data store TOML file for consumption and transformation of the NDVI variable. The variable `dates` has been highlighted for clarification. The variable `dates` in fact is a local variable in the `DataStore` class which is passed to the transformation internally by the parser.

```
[data.ndvi]
[data.ndvi.gathering]
  longname="Normalized difference vegetation index"
  source="file"
  open_with="xarray::open_dataset"
  kwargs=[""]
  path=".//pilots/portugal_pt/data/ndvi/2024.nc"
```

Figure B.15: The figure shows the parameters to be passed to the `gathering` section to load the data from the file.

the datastore class. In the case it does exist, its value is assigned to that parameter and passed to the transformation function. As an example, notice the transformation of the consumed NDVI variable shown in Figure A.14. Among the input parameters for the transformation `fill_time_dimension` is the variable `dates`, which is a local variable in the `DataStore` class. When the parser parses the `kwargs` for this transformation, before passing to the Python function (`fill_time_dimension`), the value of the variable `self.dates` in the `DataStore` class is assigned to that input parameter and passed to the transformation. Similarly, any variable defined in the pilot config file will also be passed to the reference function. However, take note that there is a variable with the same name in the `DataStore` class and the pilot TOML file; the variable value in the TOML file will have precedence.

Appendix B. Consuming data set

Appendix B.1. Consuming data set from files

In the `DataStore` class, it is possible to load the data set from a file, instead of consuming the data set from the datastore. This is especially useful when the data is static and does not require continuous updating from the data store. When loading the dataset from a file, the `source` parameter in the `gathering` is set to `file` instead of `dds`. Along with this parameter, the user must specify the path of the file (in the parameter `path`), the library and function for opening the file (in the parameter `open_with`), and the `kwargs` to be passed to the function when opening the file. These parameters are shown in the Figure B.15.

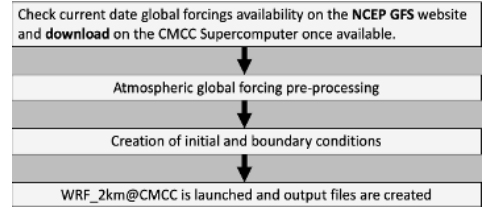


Figure C.16: WRF_2km@CMCC weather forecasts operational scheme.

Appendix C. WRF configuration

The Figure C.16 presents a simplified overview of the operational WRF_2km@CMCC configuration used for the generation of the weather forecast.

Configuration details and the sensitivity analysis that guided parameter choices as used in [21].

Appendix D. List of fire predictors

The Table D.3 shows the list of fire predictors used in the use cases. Along with the variables, their parent repository is shown as well.

Model	WRF (ARW)
Version	WRF v4.2.1
Boundary forcing	IFS ECMWF 0.05° (\approx 6 km) NCEP GFS 0.25° (\approx 27.8 km)
Lateral Boundary Condition (LBC)	Update frequency 1 h
Soil initializations	Temperature and moisture were obtained by interpolation from GFS
Horizontal resolution	0.018° (2 km), 0.01° (\approx 1.7 km)
Time step	12 seconds
N° vertical levels	60
Output frequency	1 hour
Coordinate system	Horizontal: Conformal Lambert on a latitude-longitude grid vertical: sigma-pressure
Radiation scheme	RRTMG [35]
Non-orographic gravity wave drag	The scheme includes two subgrid topography effects: gravity wave drag and low-level flow blocking [36]
Sub-grid scale orographic drag	SSO scheme [36]
Microphysics	Morrison 2-moment
Convection scheme	No cumulus parameterization
Turbulent transfer	Yamada-Joshi scheme [37]
Land surface scheme	Simplified Simple Biosphere Model [38]
Land use dataset	GlobCover2009 [39]
Time integration	3rd-order Runge Kutta
Horizontal grid	Arakawa C staggering
Spatial discretization	6th-order centered differences

Table C.2: Key features of WRF_2km@CMCC configuration

No.	Variable	Source	Aggregation
1	Normalized difference vegetation index (NDVI)	16-daily, NASA MODIS Terra [25]	16-daily, forward filled to 1-day resolution.
2	LST day & night	NASA MODIS [26]	1-day resolution
3	Dew point temperature at 2-meter	Details in Section 3.3.1	Hourly to 1-day max
4	Air temperature at 2-meter	Details in Section 3.3.1	Hourly to 1-day max
5	Surface pressure	Details in Section 3.3.1	Hourly to 1-day max
6	Total precipitation	Details in Section 3.3.1	Hourly to 1-day max
7	u&v wind speed components (10m)	Details in Section 3.3.1	Hourly to 1-day max
8	Relative humidity	Details in Section 3.3.1	Hourly to 1-day min
9	Elevation (DEM)	Copernicus [27]	Static variable
10	Slope	Derived from DEM	Static variable
11	Distance to roads	WorldPop.org [31]	Static variable
12	Distance to waterway	WorldPop.org [31]	Static variable
13	Population density	WorldPop.org [31]	Static variable
14	Corine Land Cover	Copernicus [29]	Static variable

Table D.3: List of fire predictors used in the use cases, their source, and the summary statistics applied to them.